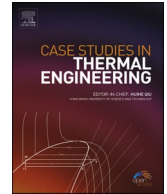




ELSEVIER

Contents lists available at ScienceDirect

## Case Studies in Thermal Engineering

journal homepage: <http://www.elsevier.com/locate/csite>

# Experimental investigation of vortex tube for reduction air inlet of a reciprocating air compressor

Anan Tempiam<sup>a</sup>, Pongsakorn Kachapongkun<sup>a,\*</sup>, Phadungsak Rattanadecho<sup>b,\*\*</sup>,  
Ratthasak Prommas<sup>a,\*\*\*</sup>

<sup>a</sup> Rattanakosin College for Sustainable Energy and Environment, Rajamangala University of Technology Rattanakosin, Nakhon Pathom, 73170, Thailand

<sup>b</sup> Center of Excellence in Electromagnetic Energy Utilization in Engineering (CEEE), Department of Mechanical Engineering, Faculty of Engineering, Thammasat University (Rangsit Campus), Pathumthani, 12120, Thailand

## ARTICLE INFO

## Keywords:

Compressed air production process  
Energy efficiency  
Air compressor inlet  
Reciprocating air compressor  
Energy savings

## ABSTRACT

A vortex tube that can be employed to lower the temperature of the inlet air of a 7.5 kW piston air compressor was designed and tested. The vortex tube reduces the air temperature by acting as a cold air generator that exchanges the temperature within the evaporator. The first step of the research method started with the design of nozzles of three sizes to be used for the vortex tubes in order to identify the most effective nozzle size, followed by the conducting of experiments to determine the energy saving procedures that can be applied to and affect the compressed air. The results of the experiments showed that the most effective design of the nozzle was able to decrease the temperature of the inlet air of the compressor by 8.3 °C. The calculation of the highest energy saving settings was 2.3% with 6.0 bar for the vortex tube and 0.0 bar for the low-pressure air tank. This savings was a result of a decrease in the pressure in the vortex tube or an increase in the low-pressure air tank's pressure level. Therefore, it was found that the energy efficiency can be improved by increasing the pressure to the vortex tube.

## 1. Introduction

Compressed air is widely used as a fluid energy for manufacturing processes in industrial plants. Compressed air systems are easy to control, quick to use, have no risk of explosion and are inexpensive, and thus facilitate car service centers, car care and many more tasks. The amount of electricity consumed by compressed air systems is 10% in Europe, the USA and Malaysia, 9.4% in China, and 9% in South Africa. In these systems, a motor in the form of an air compressor is used to produce compressed air by using the power from the electric motor to generate the fluid power. Throughout an air compressor's lifetime, the cost is 16% for the air compressor unit, 6% for the maintenance expenses and 78% for the energy to power the air compressor [1].

Compared to other forms of energy, compressed air is inefficient, due to only 19% of its energy being usable [2]. There are many losses in the system, for example the waste heat from the air compressor, leakage of air in the system, inaccurate pressure levels, an

\* Corresponding author.

\*\* Corresponding author.

\*\*\* Corresponding author.

E-mail addresses: [anan\\_nbk@hotmail.com](mailto:anan_nbk@hotmail.com) (A. Tempiam), [pongsakorn.kerd@rmutr.ac.th](mailto:pongsakorn.kerd@rmutr.ac.th), [pongsakorn.kerd@rmutr.ac.th](mailto:pongsakorn.kerd@rmutr.ac.th) (P. Kachapongkun), [ratphadu@engr.tu.ac.th](mailto:ratphadu@engr.tu.ac.th) (P. Rattanadecho), [ratthasak.pro@rmutr.ac.th](mailto:ratthasak.pro@rmutr.ac.th) (R. Prommas).

<https://doi.org/10.1016/j.csite.2020.100617>

Received 31 December 2019; Received in revised form 25 February 2020; Accepted 26 February 2020

Available online 29 February 2020

2214-157X/© 2020 Rajamangala University of Technology Rattanakosin. Published by Elsevier Ltd. This is an open access article under the CC

BY license (<http://creativecommons.org/licenses/by/4.0/>).

## Nomenclature

$\Delta T_c$	temperature difference between the inlet and the cold outlet
$\Delta T_h$	temperature difference between the inlet and the hot outlet
$\gamma$	specific heat ratio
$\rho$	density (kg/m <sup>3</sup> )
$\eta_{ac}$	efficiency of air compressor (%)
$A$	cross-sectional area (m <sup>2</sup> )
C.O.P.	coefficient of performance
$C_p$	specific heat at constant pressure (kJ/kg K)
$\dot{m}$	mass flow rate (kg/s)
$\dot{m}_c$	mass flow rate for cold stream (kg/s)
$\dot{m}_h$	mass flow rate for hot stream (kg/s)
$\dot{m}_i$	inlet mass flow rate (kg/s)
$n$	polytropic index
$P$	air pressure (bar)
$P_0$	ambient pressure (bar)
$P_1$	outlet pressure of air compressor (°C)
$P_2$	pressure in low pressure tank (bar)
$P_3$	inlet pressure to vortex tube (bar)
$P_c$	cold outlet pressure (bar)
$P_i$	inlet pressure (bar)
$Q_c$	thermal cooling load (kW)
$Q_h$	thermal heating load (kW)
$R$	gas constant (kJ/kg K)
$T$	air temperature (°C)
$T_0$	ambient temperature (°C)
$T_1$	inlet air temperature to air compressor (°C)
$T_2$	outlet air temperature of air compressor (°C)
$T_3$	inlet air temperature to vortex tube (°C)
$T_4$	outlet air temperature of vortex tube (°C)
$T_5$	outlet air temperature of evaporator (°C)
$T_c$	cold outlet temperature (°C)
$T_h$	hot outlet temperature (°C)
$T_i$	inlet temperature (°C)
$\mu_c$	cold mass fraction
$v$	air velocity (m/s)
$\dot{V}$	volume flow rate (m <sup>3</sup> /s)
$W_{ac,I}$	energy input of air compressor (kJ/kg)
$\dot{W}_{ac,I}$	energy input of air compressor (kW)
$\dot{W}_{ac,O}$	energy output of air compressor (kW)
$W_i$	work input rate (kW)

excessively large air compressor, inappropriate pressure throughout the system or control of the air compressor, etc. [3,4]. Thus, it is necessary to implement energy conservation in compressed air systems for industrial purposes because the energy consumption represents a significant cost in the production process. Based on the abovementioned factors causing the loss of energy in compressed air systems, there is a possibility of achieving a reduction in the loss of energy loss from the air compressor by lowering the air temperature at the inlet of the air compressor through the use of a vortex tube and thereby, increasing its efficiency. Therefore, the design and testing of vortex tubes for use in reducing the temperature at the compressor's air inlet was the objective of this research. Because Thailand is a tropical country, the air temperature in the housing of the air compressors is high. as a consequence of the heat from the sunlight entering the building where the air compressors are installed via the roof [5–7] and walls [8,9]. Moreover, the machine's operation transfers the generated heat to the housing of the compressors [10–12].

In previous research, several interesting methods of cooling the inlet air entering air compressors have been investigated. As mentioned by Refs. [13,14], the inlet fogging system using two-fluid nozzles was tested in order to determine the important parameters including the air supply pressure, temperature and water flow rate. Other methods, for example direct evaporative pad cooling, were also implemented in poultry houses [15] as well as a thermo-electric module for cooling a dual processor computer and air cooler fan [16,17].

### 1.1. Vortex tubes

A vortex tube is a device involving the phenomenon of separation of air currents with different temperatures that was discovered accidentally by Georges Ranque, a French physicist, while conducting an experiment. As a result, vortex tubes can produce currents of cool and hot air simultaneously through the compressed air flow in the pipe. The compressed air enters a T-shaped cylindrical pipe having a nozzle in the center close to the inlet pipe, in which hot currents are produced and flow out of one exit of the pipe and a cold stream of air escapes from the other exit, a process that Ranque, who patented it in the United States in 1934, described in his published research [18]. In 1947, Rudolf Hilsch, a German researcher, conducted a study and published his findings that provided information about improving the composition, structure and size of the pipes and described the working conditions that have an impact on the performance of vortex pipes. Moreover, the potential for utilizing this device for the purpose of spot cooling was suggested [19–22]. Over time, there has been increasing interest in vortex tubes from researchers conducting theoretical studies that explain the phenomena of temperature separation and operation as well as those who are investigating the effective applications of vortex pipes [23].

As seen in Fig. 1, the operation of a vortex tube begins with the flow of the high-pressure compressed air in a tangential line through the nozzle into the tube, which involves strong circular movement at high rpm as well as centrifugal force. Consequently, there is an expansion of the fluid within the pipe, which causes a decrease in the pressure. This results in a difference in the fluid's velocity in the center of the pipe, and the outer edge close to the pipe wall receives a kinetic energy transfer from the flow of fluid in the center of the pipe to the fluid along the pipe wall. The temperature is then lowered by the air flow in the central axis, whereas the air current along the pipe wall increases in temperature and causes the separation of the layer of thermal energy to occur inside the pipe. Furthermore, the structure of the pipe includes a central orifice opening and a cone-shape valve located at the outlet of the pipe where the release of the hot air occurs, causing lower temperature air currents in the core of the pipe that move back and forth to the central orifice and exits the vortex tube at the end opposite to that of the hot air current [24,25].

The temperatures of the hot air and the reduced temperature cold air are calculated using Equations (1) and (2) [26].

$$\Delta T_c = T_i - T_c \quad (1)$$

$$\Delta T_h = T_h - T_i \quad (2)$$

where  $\Delta T_c$  indicates the temperature of the cold air that is decreased from the temperature of the compressed air inlet ( $^{\circ}\text{C}$ ),  $\Delta T_h$  is the increase of temperature of the hot air from the compressed air inlet's temperature ( $^{\circ}\text{C}$ ),  $T_i$  is the temperature at the compressed air inlet ( $^{\circ}\text{C}$ ),  $T_c$  is the cold air temperature ( $^{\circ}\text{C}$ ), and  $T_h$  is the hot air temperature ( $^{\circ}\text{C}$ ).

The calculations of the thermal cooling load ( $Q_c$ ) and thermal heating load ( $Q_h$ ) were performed in accordance with the following equations [27]:

$$Q_c = \dot{m}_c C_p (T_i - T_c) \quad (3)$$

$$Q_h = \dot{m}_h C_p (T_h - T_i) \quad (4)$$

The most commonly used variables in the evaluation of the efficiency of vortex tubes are the cold mass fraction ( $\mu_c$ ) and the exiting cold mass flow rate ( $\dot{m}_c$ ), which is compared with the air inlet mass flow rate ( $\dot{m}_i$ ) [28].

$$\mu_c = \frac{\dot{m}_c}{\dot{m}_i} \quad (5)$$

The Coefficient of Performance (C.O.P.) of a vortex tube is defined as the ratio of the cooling rate per energy used in the cooling based on the same principles of the isentropic expansion for ideal gas as in Equation (6) [29,30]:

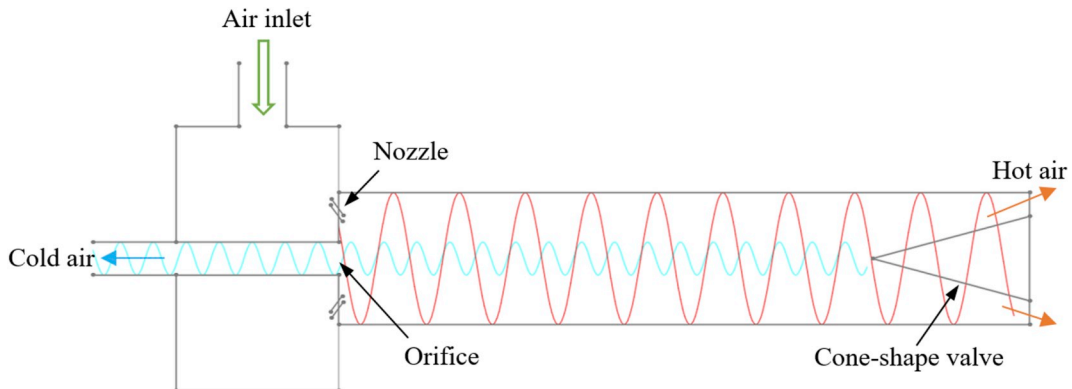


Fig. 1. Working principle of a vortex tube.

$$C.O.P = \frac{Q_c}{W_i} = \frac{\dot{m}_c C_p (T_i - T_c)}{\dot{m}_i \times \frac{\gamma}{\gamma-1} \times RT_i \left[ \left( \frac{P_2}{P_1} \right)^{\frac{\gamma-1}{\gamma}} - 1 \right]} \tag{6}$$

1.2. Air compressors

A reciprocating stroke compressor is a type of air compressor that compresses the air in a cylinder by transferring it upward at the top dead center (TDC) and the suction of the external air when moving it downward at the bottom dead center (BDC) of the cylinder, as illustrated in Fig. 2(a).

The explanation of the operation of an air compressor is provided by the diagram showing the relationship between the pressure and the volume (P-v diagram) of the air inside the cylinder, as seen in Fig. 2(b). The cycle of this process includes [31] (1-2) the compressed air that is processed from pressure  $P_1$  to pressure  $P_2$  as a polytropic process ( $Pv^n = C$ ), (2-3) the process of removing the air from the cylinder at constant pressure ( $P_2 = P_3$ ), (3-4) the process of expanding the compressed air in the piston head gap as a polytropic process ( $Pv^n = C$ ), and (4-1) the process of pulling the air into the cylinder at constant pressure ( $P_4 = P_1$ ).

The rate of the air flow entering the air compressor ( $\dot{V}$ ) is calculated [32] using Equation (7), where  $A$  represents the cross-sectional part of the air tube and  $v$  indicates the speed of the air,

$$\dot{V} = Av \tag{7}$$

The mass flow rate of the air into the compressor ( $\dot{m}$ ) is another parameter, which is calculated by Equation (8), in which  $\rho$  is the air density that is determined with Equation (9),

$$\dot{m} = \rho \dot{V} \tag{8}$$

$$\rho = \frac{P}{RT} \tag{9}$$

The energy consumption of the theoretical air compressor is calculated based on Equation (10), where  $T_1$  is the temperature of the inlet air,  $P_1$  is the absolute air pressure entering the compressor,  $P_2$  is the absolute air pressure exiting the compressor,  $n$  represents the polytropic index,  $R$  indicates the air constant, and  $W_{ac,I}$  is the energy consumption per unit mass of the air compressor [33],

$$W_{ac,I} = \frac{n}{n-1} R T_1 \left[ \left( \frac{P_2}{P_1} \right)^{\frac{n-1}{n}} - 1 \right] \tag{10}$$

The energy is used by the compressed air in units of kW ( $\dot{W}_{ac,I}$ ), in which, if they were calculated with a mass flow rate of air into the air compressor ( $\dot{m}$ ), it was found that

$$\dot{W}_{ac,I} = \dot{m} W_{ac,I} \tag{11}$$

The calculation of the hydraulic power is as follows [32]:

$$\dot{W}_{ac,O} = \dot{V} P_0 \ln \left( \frac{P_1}{P_0} \right) \tag{12}$$

The calculation of the efficiency of the compressed air ( $\eta_{ac}$ ) is performed with Equation (13) [33]:

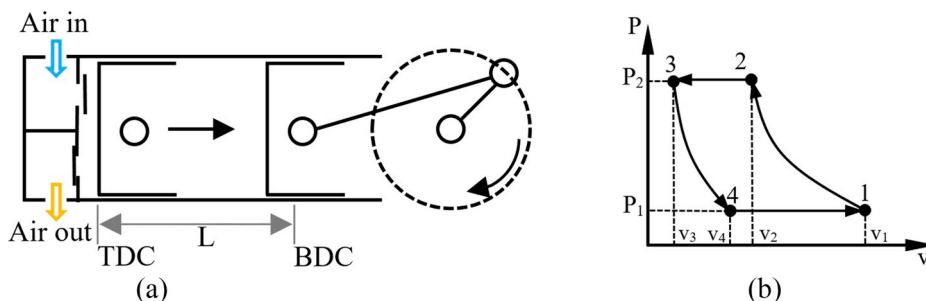


Fig. 2. Principle of a reciprocating air compressor.

$$\eta_{ac} = \frac{\dot{W}_{ac,O}}{\dot{W}_{ac,I}} \quad (13)$$

## 2. Experimental set up

Fig. 3 illustrates the design of the vortex tube studied in this work. As can be seen, the length of the hot air section is  $L_h = 4D$ , the length of cold air section is  $L_c = 0.5D$ , and the diameter  $D$  was set at 24 mm. The investigation included three types of nozzles, in which the cold section diameter,  $d_c/D$ , and  $z$ , which represents the groove depth for the different nozzle sizes, were varied.

The design of the vortex tube is aimed at the reduction of the temperature at the compressor's air inlet by operating in combination with the evaporator, as seen in Fig. 4, in which the exchange of the temperature of the air in the compressor with the cold air being released by the Vortex tube occurs. The evaporator was constructed with 36 runs of 8-mm diameter coiled aluminum tubes having 128 fins. As a result, this research includes three sections: optimization of the cold-mass fraction for the various nozzle sizes, identification of the temperature changes caused by the vortex tube, and calculation of the system's energy-based gains.

### 2.1. Control of the hot air volume of the vortex tube to determine the most effective cold mass fraction for each nozzle size

The process, as seen in Fig. 5, starts with the intake of air into the evaporator from the atmosphere at an ambient temperature ( $T_0$ ), which is used to exchange the temperature with the cooling air ( $T_4$ ) released from the vortex tube. Then, the cooled air is transferred to the air compressor, which compresses it into the high-pressure air tank in a range of 6.0–8.0 bar. Meanwhile, the air in the storage tank is sent to the vortex tube for removal of moisture via the air dryer. Furthermore, the pressure is maintained at 6.0 bar by using a pressure regulator, and the measurement of the flow of compressed air is carried out using a flow meter before it enters the vortex tube. There are two parts to the compressed air of the vortex tube, the first of which is when the cooling air flows through the air flow meter and enters the evaporator system for the exchange of temperature with the compressor's air inlet and exits into the atmosphere via the low-pressure tank. The second part involves the thermal air also flowing from the vortex tube through the thermal air intake valve, followed by being released into the atmosphere via the low-pressure tank.

The set-up of the experiment was conducted by connecting the six temperature sensors, which are as follows:  $T_0$ ,  $T_1$ ,  $T_2$ ,  $T_3$ ,  $T_4$  and  $T_5$ , and connecting the flow meter sensor and pressure sensor as  $P_1$  to the data logger. Nozzle size 1 was then fitted to the vortex tube, and clockwise adjustment of the cone-shape valve was done until reaching the maximum point. The pressure regulator was set at 6.0 bar, then the shut-off valve was opened and the compressed air released into the vortex tube. After counter-clockwise adjusting of the cone-shape valve, for the recording of the  $Q_i$  and  $Q_c$  values, the cold mass fraction was determined by Equation (5), which gave  $\mu_c = 0.9$ . When the temperature  $T_4$  was stable, the recording could begin. Following the air compressor's completion of one On/Off cycle, the recording was stopped. Further adjustment of the cone-shape valve was conducted in order to be in line with the cold mass fractions of  $\mu_c$  0.8 to 0.1. Nozzles 2 and 3 were also tested using these steps.

The most effective setting of the cone-shape valve was considered to be the one that produced the highest  $Q_c$  and  $C.O.P.$  values, which were identified using the temperature readouts with the previously mentioned equations. These settings were applied in the

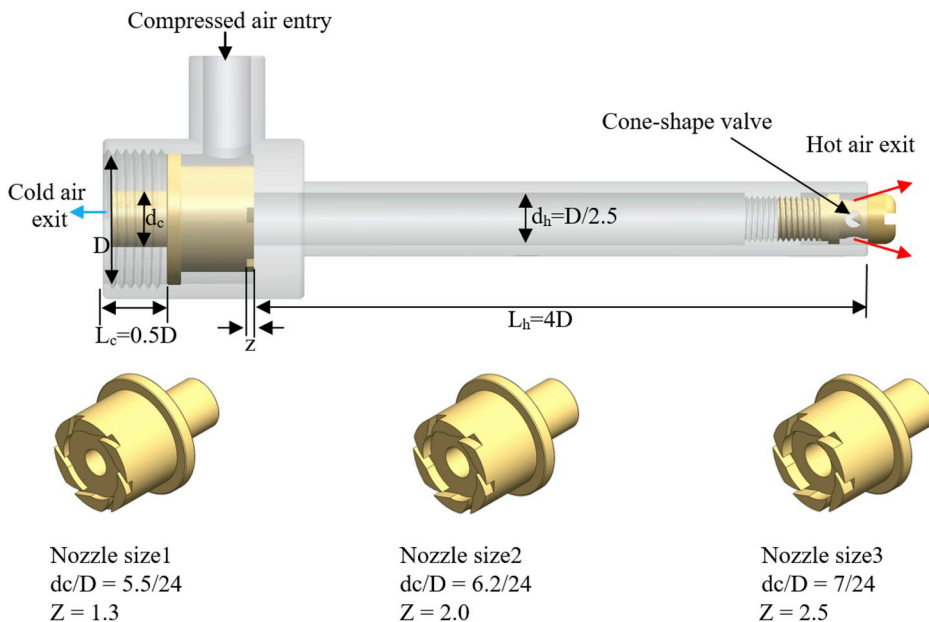


Fig. 3. Vortex tube model.

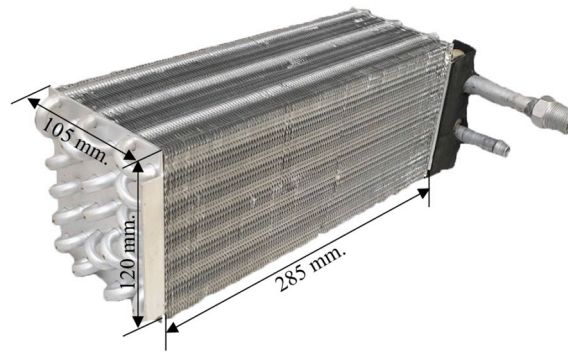


Fig. 4. Evaporator size for the experiment.

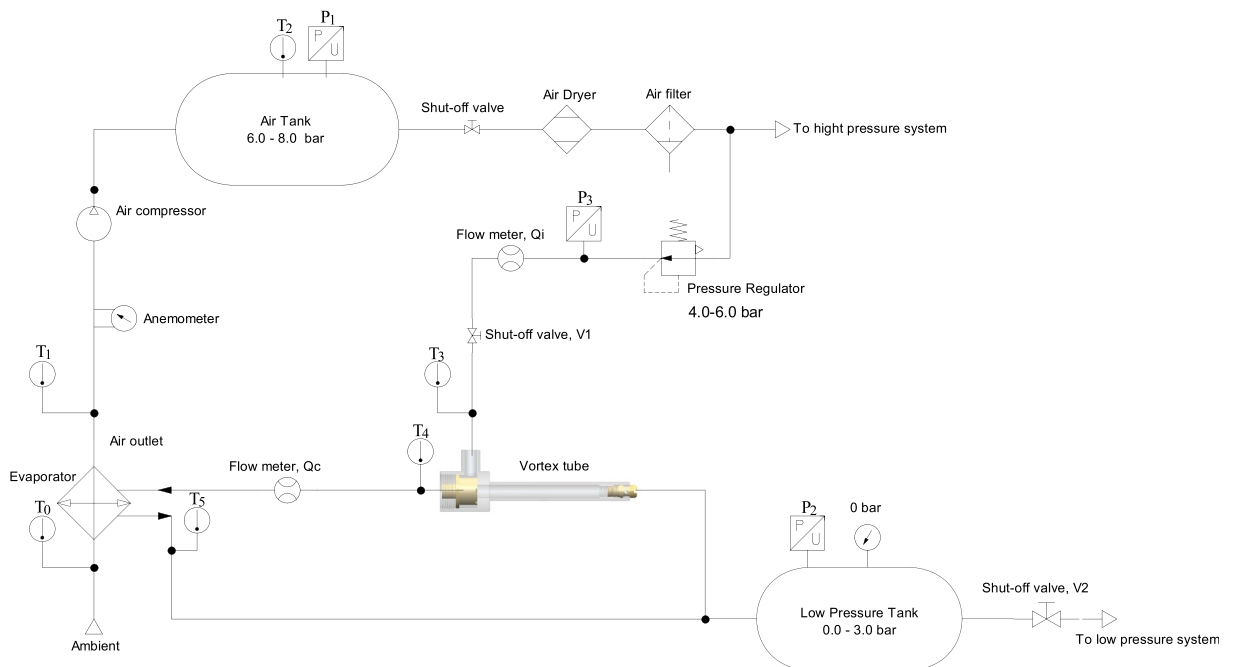


Fig. 5. Schematic showing the vortex tube and intake air flow of the air compressor.

subsequent sections.

## 2.2. Temperature differences achieved by vortex tube at 6.0 bar with low-pressure air tank at 0.0–3.0 bar

The previously performed experiment identified the appropriate cone-shape valve setting, and the most suitable nozzle size for the evaporator in this research was also shown by the results. The first step involved the simulation of the situation in which the low-pressure air employed in the production process is within the pressure range of 0.0–3.0 bar.

As seen in in Fig. 5, the experiment was conducted using a similar method to the experiment in section 2.1. However, there was a different process concerned with the thermal air and the cooling air exiting the vortex tube, which were stored for use in the low pressure coolant tanks at an operating pressure range at 0.5–3.0 bar instead of being discharged into the atmosphere.

The setting up of the experiment included connecting the temperature sensors at  $T_0$ ,  $T_1$ ,  $T_2$ ,  $T_3$ ,  $T_4$  and  $T_5$ , the two flow meters, and the three pressure sensors at  $P_1$ ,  $P_2$  and  $P_3$  in combination with the data logger, the nozzle size 1 being placed in the vortex tube, and the adjustment of the cone-shape valve to the most appropriate position and the pressure regulator at 6.0 bar. In order to let the compressed air enter the vortex tube, shut-off valve V1 was opened, and to measure the pressure in the low-pressure air tank at 0.5 bar, shut-off valve V2 was opened. When the temperature at  $T_4$  stabilized, the recording was started, and after running one cycle of the compressor, it was stopped. For the purpose of pressurizing the low-pressure tank from 0.5 to 3.0 bar in 0.5 bar steps, the shut-off valve V2 was opened, and each step was recorded. Upon completion, the procedure was repeated using nozzle sizes 2 and 3.

Analysis of the recorded data was performed in order to discover the differences in temperature between the temperature of the

environment ( $T_0$ ) and the temperature of the air flow into the compressor, which was exchanged with the evaporator and ( $T_1$ ), in order to determine the nozzle size that is the most suitable for the evaporator’s temperature exchanger to be used in the final section of this study.

2.3. Energy saving value of an air compressor with vortex tube at 4.0 to 6.0 bar and a low-pressure air tank at 0.5 to 3.0 bar

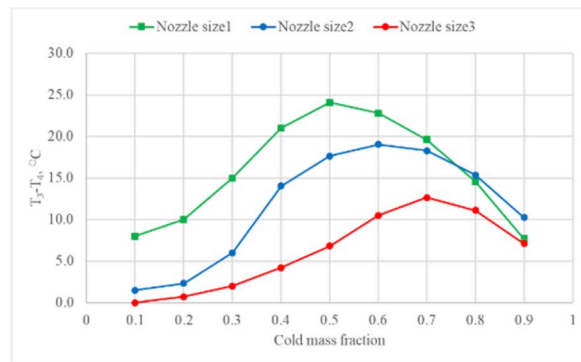
In part 2.2, the previous section, the size of the nozzle that was most appropriate for the investigation to examine the air compressor’s energy saving value was identified. In the next step, the operations in the polytropic compression process, as determined by Equations (10) and (11), were calculated. The volume of flow and the mass flow rate of air into the air compressor are required, as seen in Equations (7) and (8), respectively. The energy saving effect that occurs can be calculated from the experiment on the air temperature of the reduced compressed air in comparison to the air temperature in the air compressor at 30 °C. The air intake temperature of the reduced compressed air can be calculated under various conditions of the compressed air pressure settings applied to the vortex tube from 4.0 to 6.0 bar. Incremental adjustments of 0.5 bar and the low-pressure air tank pressure settings in order to induce the low-pressure operations at 0.5 to 3.0 bar were performed, respectively.

2.4. Uncertainty analysis

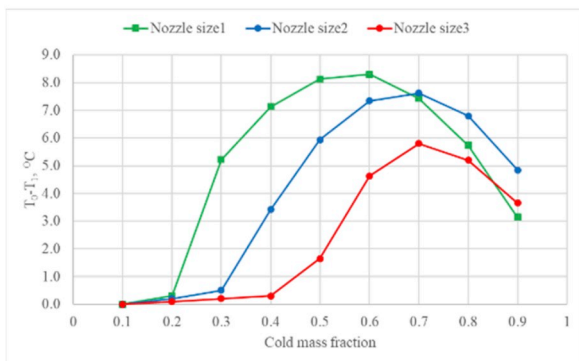
It is essential to conduct an assessment of the uncertainty when the experimental results are evaluated. In this research, the uncertainty was evaluated based on the method that has been proposed [34]. Each variable  $x_1, x_2, x_3 \dots x_n$  has a specific function that provides the result  $m$ . If the uncertainty of each variable is  $w_1, w_2, w_3 \dots w_n$  and all are identified by the same odds, the uncertainty of this potential  $w_m$  result can occur, which can be represented by Equation (14):

$$w_m = \left[ \left( \frac{\partial m}{\partial x_1} w_1 \right)^2 + \left( \frac{\partial m}{\partial x_2} w_2 \right)^2 + \dots + \left( \frac{\partial m}{\partial x_n} w_n \right)^2 \right]^{1/2} \tag{14}$$

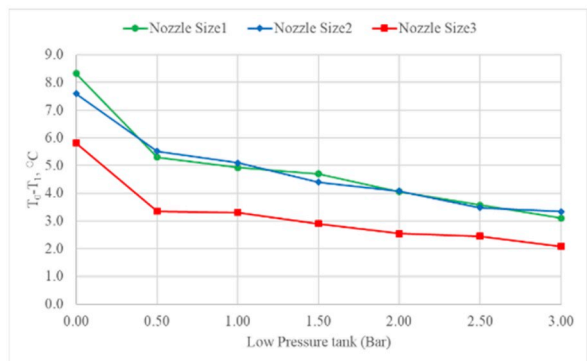
In this research, the calculated volume flow rate, mass flow rates and energy consumption per unit mass of the air compressor using appropriate tools were previously described. Error assessment to evaluate the maximum uncertainty in the experimental results was performed using Equation (14), which found that the uncertainty occurs in up to 3.2% of all of the variables mentioned.



(a)  $T_3-T_4$



(b)  $T_2-T_1$



(c)  $(T_0-T_1)$  in low-pressure tank at 0.5 – 3.0 bar

Fig. 6. Effects of the temperature differences.

### 3. Results and discussion

#### 3.1. Calculations of the results regarding the thermal air were conducted in order to identify the cone-shape valve settings for control of the cold mass fractions of the vortex tube

Calculating that position provides the highest difference of temperature between the temperature of the compressed air intake and the outlet of the cooling air ( $T_3-T_4$ ). As shown in Fig. 6(a), the highest value for nozzle size 1 was 24.1 °C, at the position of  $\mu_c = 0.5$ , while those of nozzles size 2 and size 3 were 19.0 °C and 12.7 °C, at the positions of  $\mu_c = 0.6$  and 0.7, respectively. Table 1 displays the energy values of the cooling air and the C.O.P. of all of the nozzle sizes.

The results confirmed the possibility of exchanging the temperature with the air inlet of the compressor through the evaporator by using the cool air from the vortex tube. It was found that there are differences in the air compressor inlet's temperature and the environmental temperature ( $T_0-T_1$ ) as a result of the three sizes of nozzles. These differences are shown in Fig. 6(b), in which it can be seen that the value of nozzle size 1 for  $T_0-T_1$  was the highest at 8.3 °C, at the position  $\mu_c = 0.6$ , while the highest values of nozzles size 2 and size 3 were at 7.6 °C and 5.8 °C, at the position  $\mu_c = 0.7$ , respectively. In contrast, with regard to the different temperatures at  $T_0-T_1$  and  $T_3-T_4$ , it was revealed that the highest nozzle size 1 and 2 values occurred at a different position of  $\mu_c$ , where nozzle size 1 showed the highest  $Q_c$  for the cold mass fraction at 0.6 and nozzle size 2 for  $Q_c$  at the cold mass fraction at 0.7.

#### 3.2. Results for the air temperature in the compressed air under the vortex tube compressed air condition of 6.0 bar and the pressure in the low-pressure air tank at 0.0–3.0 bar

Comparison of the three nozzle sizes was conducted by producing the cooling air in the evaporator and exchanging the temperature with the ambient air ( $T_0-T_1$ ). In the first step, the hot and cooling air flowed out of the vortex tube and entered the air-cooling tank. Following this, the low pressure was applied by implementing the low-pressure compressed air for a variety of processes. Then, the compressed air at a low-pressure in the range of 0.0 to 3.0 bar, which was adjusted in the constant low-pressure air tank starting at 0.0 and continuing to 0.5, 1.0, 1.5, 2.0, 2.5 and 3.0 bar, was required. The differences between the air compressor entrance temperature and the environmental temperature were compared, and the results are shown in Table 2 and Fig. 6(c).

The results as seen in Fig. 6(c) demonstrate that in the case of each nozzle size, there are differences between the temperature of the air compressor inlet and the environmental temperature ( $T_0-T_1$ ). This reduction is linear when the pressure in the low-pressure air tank is 0.5 bar or higher. Based on the results regarding the size of the nozzles, nozzle size 3 was found to have the lowest temperature difference between the air compressor inlet and the ambient temperature when applying the highest compressed air flow rate, whereas there are larger differences in temperature with nozzle sizes 1 and 2, but the trend is similar. With regard to the ratio between the temperature differences of the air compressor inlet and the environmental temperature, a good C.O.P. could be achieved. For use with the evaporator in this study, nozzle 1 was identified as the most appropriate.

#### 3.3. Identifying the energy saving value of the air compressor, which was set for the compressed air conditions with the vortex tube at 4.0–6.0 bar and the pressure in the low-pressure air tank at 0.5–3.0 bar

This experiment was conducted in order to examine the relationship regarding the differences in temperature between the air compressor inlet and the ambient temperature as ( $T_0-T_1$ ), which includes the pressure of the compressed air in the vortex tube and the low-pressure air tank's pressure level by setting the compressed air in the vortex tube at pressures of 4.0, 4.5, 5.0, 5.5 and 6.0 bar and the low-pressure air tank's level of pressure at 0.0, 0.5, 1.0, 1.5, 2.0, 2.5 and 3.0 bar. Fig. 7 displays the results of the experiment.

Regarding the data in Fig. 7(a), the temperature differences between the air compressor inlet and the ambient temperature ( $T_0-T_1$ ) were recorded, and it can be seen that there was a tendency for them to increase linearly as a result of the increased pressure in the compressed vortex tube. However, regarding the low-pressure air tank, a higher pressure was found; thus, the differences in temperature between the air compressor inlet and the environmental temperature ( $T_0-T_1$ ) shows a tendency to decrease. In summary, if the pressure of the compressed air in the vortex tube is high and the low-pressure air tank's pressure is low, the high temperature difference between the air compressor inlet and the environmental temperature ( $T_0-T_1$ ) is produced. Conversely, if the compressed air pressure in

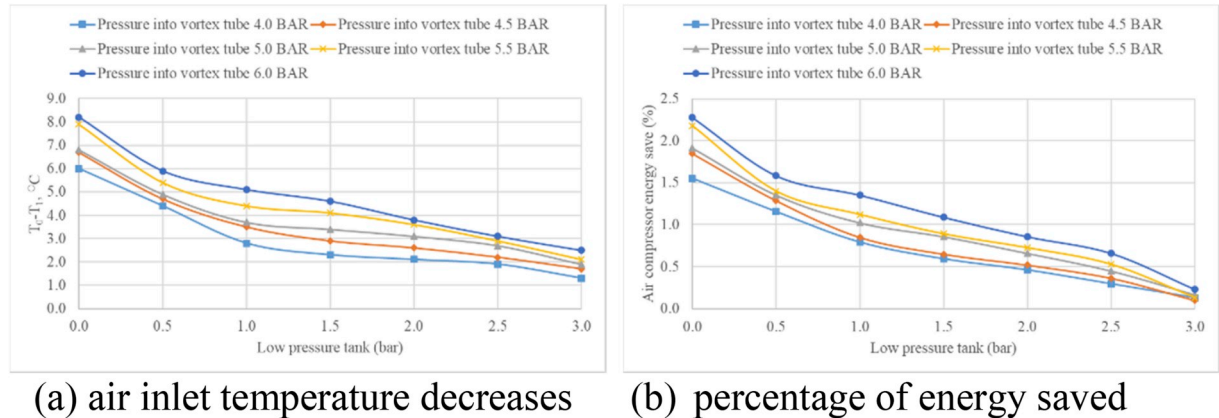
**Table 1**  
Results of tests of all nozzle sizes.

$\mu_c$	Nozzle size 1				Nozzle size 2				Nozzle size 3			
	$T_0-T_1$ (°C)	$T_3-T_4$ (°C)	$Q_c$ (W)	C.O.P.	$T_0-T_1$ (°C)	$T_3-T_4$ (°C)	$Q_c$ (W)	C.O.P.	$T_0-T_1$ (°C)	$T_3-T_4$ (°C)	$Q_c$ (W)	C.O.P.
0.1	0.0	8.0	39.4	0.004	0.0	1.5	9.2	0.001	0.0	0.0	0.0	0.000
0.2	0.3	10.0	99.2	0.009	0.2	2.3	28.2	0.002	0.1	0.7	9.5	0.001
0.3	5.2	15.0	226.9	0.021	0.5	6.0	111.8	0.008	0.2	2.0	40.9	0.003
0.4	7.1	21.0	432.6	0.039	3.4	14.0	358.4	0.026	0.3	4.2	115.2	0.007
0.5	8.1	<b>24.1</b>	627.1	0.057	5.9	17.6	569.9	0.042	1.7	6.8	235.3	0.015
0.6	<b>8.3</b>	22.8	<b>708.9</b>	<b>0.065</b>	7.3	<b>19.0</b>	742.6	0.054	4.6	10.5	441.4	0.029
0.7	7.4	19.6	704.2	0.064	<b>7.6</b>	18.3	<b>829.6</b>	<b>0.061</b>	<b>5.8</b>	<b>12.7</b>	<b>625.1</b>	<b>0.041</b>
0.8	5.7	14.6	587.5	0.054	6.8	15.3	787.6	0.057	5.2	11.1	623.5	0.041
0.9	3.1	7.7	339.0	0.031	4.8	10.2	580.3	0.042	3.7	7.1	442.9	0.029

**Table 2**

Decrease in the temperature of the air entering the compressor at the pressure in the low-pressure air tank at 0.0–3.0 bar.

Low pressure air tank (bar)	$T_0-T_1$ (°C)		
	Nozzle size 1	Nozzle size 2	Nozzle size 3
0.00	8.3	7.6	5.8
0.50	5.3	5.5	3.4
1.00	4.9	5.1	3.3
1.50	4.7	4.4	2.9
2.00	4.1	4.1	2.5
2.50	3.6	3.5	2.4
3.00	3.1	3.3	2.1

**Fig. 7.** Air inlet temperature decreases and percentage of energy saved.

the vortex tube is low and the pressure in the low-pressure air tank is high, it will lead to a low temperature difference between the air compressor inlet and the ambient temperature ( $T_0-T_1$ ).

The result of these values was a reduction in the temperature of the air that entered the compressor, a comparison of which is made to the compressor in operation at an ambient temperature of 30 °C. Following this, the calculation of the energy savings effect on the air compressor can be conducted to provide a percentage of the energy saved, as shown in Fig. 7(b). It was found that the highest level of savings was 2.3% when the pressure of the compressed air in the vortex tube was 6.0 bar, and the low-pressure air tank's level was 0.0 bar. This dropped to 0.2% as the pressure in the low-pressure tank was increased to 3.0 bar. There was also a decrease in this effect when the pressure in the vortex tube dropped to 4.0 bar, with 1.6% and 0.1% being recorded in the set-up of the low-pressure tank at 0.0 bar and 4.0 bar, respectively. The resulting energy savings are linear, similar to the ( $T_0-T_1$ ) values.

#### 4. Conclusions

The experiments involving the design of a vortex tube for the reduction of the temperature at the compressor's air inlet using a heat exchanger evaporator were completed. It was found that, in this study, nozzle size 1 is the most appropriate for the evaporator because, with the method of adjustment of the cone-shape valve to obtain the cold mass fraction, the results showed that the best value was 0.6. By applying this setup, the temperature of the compressor's air inlet was reduced by up to 8.3 °C, and the value of the *C.O.P.* was 0.065, which indicates that the energy savings for the air compressor reached 2.3%. This was accomplished with the settings of 6.0 bar for the compressed air pressure to the vortex tube and 0.0 bar for the working pressure of the low-pressure air tank. Thus, the working pressure at the low-pressure air tank at 0.0 bar can help to reduce the compressor's energy consumption to the minimum when a compressed air pressure of 4.0 bar is applied to the vortex tube. Moreover, the pressure of 3.0 bar in the low-pressure air tank resulted in an 0.1% savings effect. In conclusion, if a high level of pressure is utilized in the vortex tube and the low-pressure air tank's pressure is maintained at a low level, the goal of maximum savings can be achieved and, in contrast, the opposite of this is also true.

#### Declaration of competing interest

The author and all co-author not have conflict of Interest.

#### CRedit authorship contribution statement

Anan Tempiam: Conceptualization, Writing - original draft. Pongsakorn Kachapongkun: Writing - original draft,

Conceptualization. **Ratthasak Prommas**: Conceptualization, Writing - original draft.

## Acknowledgements

The authors are grateful to RCSEE at the Rajamangala University of Technology Rattanakosin (RMUTR), Thailand for providing the financial and resource support of this work and Rajamangala University of Technology Phranakhoon (RMUTP) for providing the materials used in the experiment and the resource support of this work as well as the Thailand Research Fund, Thailand (contract No. RTA 5980009) and the Thailand government budget grant that contributed financial support for this study.

## Appendix A. Supplementary data

Supplementary data to this article can be found online at <https://doi.org/10.1016/j.csite.2020.100617>.

## References

- [1] R. Saidur, N.A. Rahim, M. Hasanuzzaman, A review on compressed-air energy use and energy savings, *Renew. Sustain. Energy Rev.* 14 (2010) 1135–1153, <https://doi.org/10.1016/j.rser.2009.11.013>.
- [2] Chris Y. Yuan, Teresa Zhang, Arvind Rangarajan, David Dornfeld, Bill Ziemba, Rod Whitbeck, A decision-based analysis of compressed air usage patterns in automotive manufacturing, *J. Manuf. Syst.* 25 (4) (2006) 293–300, [https://doi.org/10.1016/S0278-6125\(06\)80241-4](https://doi.org/10.1016/S0278-6125(06)80241-4).
- [3] Min Xiang, Yang Xu, Chuan-yong Li, Yang Liu, Yi Zhang, Energy conservation co-operative control mechanism based on gray prediction for structural air compressor, *J. Autom. Construct.* 30 (2013) 184–190, <https://doi.org/10.1016/j.autcon.2012.10.002>.
- [4] Ming Yang, Air compressor efficiency in a Vietnamese enterprise, *J. Energy Pol.* 37 (2009) 2327–2337, <https://doi.org/10.1016/j.enpol.2009.02.019>.
- [5] R. Prommas, S. Phiraphat, P. Rattanadecho, Energy and exergy analyses of PV roof solar collector, *Int. J. Heat Technol.* 37 (1) (2019) 303–312, <https://doi.org/10.18280/ijht.370136>.
- [6] D. Nonthiworawong, P. Rattanadecho, R. Prommas, Energy and exergy analysis of low-cooling in building by using light-vent pipe, *Sci. Tech.* 24 (1) (2019) 41–53.
- [7] S. Phiraphata, R. Prommas, W. Puangsombut, Experimental study of natural convection in PV roof solar collector, *Int. Commun. Heat Mass Tran.* 89 (2017) 31–38, <https://doi.org/10.1016/j.icheatmasstransfer.2017.09.022>.
- [8] R. Prommas, T. Rungsakthaweekul, Effect of microwave curing conditions on high strength concrete properties, *Energy Procedia* 56 (2014) 26–34, <https://doi.org/10.1016/j.egypro.2014.07.128>.
- [9] R. Prommas, P. Rattanadecho, W. Jindarat, Energy and exergy analyses in drying process of non-hygroscopic porous packed bed using a combined multi-feed microwave-convective air and continuous belt system (CMCB), *Int. Commun. Heat Mass Tran.* 39 (2012) 242–250, <https://doi.org/10.1016/j.icheatmasstransfer.2011.10.004>.
- [10] R. Prommas, Theoretical and experimental study of heat and mass transfer mechanism during convective drying of multi-layered porous packed bed, *Int. Commun. Heat Mass Tran.* 38 (7) (2011) 900–905, <https://doi.org/10.1016/j.icheatmasstransfer.2011.03.031>.
- [11] R. Prommas, P. Keangin, P. Rattanadecho, Energy and exergy analyses in convective drying process of multi-layered porous packed bed, *Int. Commun. Heat Mass Tran.* 37 (2010) 1106–1114, <https://doi.org/10.1016/j.icheatmasstransfer.2010.06.013>.
- [12] S. Sopida, N. Dithra, R. Phadungsak, R. Prommas, Experimental investigation of attic heat gain reduction and indoor illuminance using a light-vent pipe, *Int. J. Heat Technol.* 37 (4) (2019) 1171–1179, <https://doi.org/10.18280/ijht.370427>.
- [13] A. Suryan, Y.K. Yoon, D.S. Kim, H.D. Kim, Experimental investigations on impaction pin nozzles for inlet fogging system, *J. Mech. Sci. Technol.* 259 (4) (2011) 839–845, <https://doi.org/10.1007/s12206-011-0143-3>.
- [14] A. Suryan, D.S. Kim, H.D. Kim, Experimental study on the inlet fogging system using two-fluid nozzles, *J. Therm. Sci.* 19 (2) (2010) 132–135, <https://doi.org/10.1007/s11630-010-0132-3>.
- [15] A. Lakhni, M. Mahdaoui, A.B. Abdellah, K. Anoune, M. Bakhouya, H. Ezbakhe, Performance analysis and optimal parameters of a direct evaporative pad cooling system under the climate conditions of Morocco, *Case Stud. Therm. Eng.* 13 (2019), <https://doi.org/10.1016/j.csite.2018.11.013>, 100362.
- [16] S. Wiriyasart, C. Hommalee, P. Naphon, Thermal cooling enhancement of dual processors computer with thermoelectric air cooler module, *Case Stud. Therm. Eng.* 14 (2019), <https://doi.org/10.1016/j.csite.2019.100445>, 100445.
- [17] S. Wiriyasart, P. Naphon, C. Hommalee, Sensible air cool-warm fan with thermoelectric module systems development, *Case Stud. Therm. Eng.* 13 (2019), <https://doi.org/10.1016/j.csite.2018.100369>, 100369.
- [18] G.J. Ranque, Method and apparatus for obtaining from a fluid under pressure two currents of fluids at different temperatures, *U. S. Pat.* 1952281 (1934)..
- [19] N. Li, Z.Y. Zeng, Z. Wang, X.H. Han, G.M. Chen, Experimental study of the energy separation in a vortex tube, *Int. J. Refrig.* 55 (2015) 93–101, <https://doi.org/10.1016/j.jrefrig.2015.03.011>.
- [20] Kun Chang, Qing Li, Gang Zhou, Qiang Li, Experimental investigation of vortex tube refrigerator with a divergent hot tube, *Int. J. Refrig.* 34 (2011) 322–327, <https://doi.org/10.1016/j.jrefrig.2010.09.001>.
- [21] A. Maheswaran, S. Purusothaman, C. Shravanth Bharadwaj, Design of vortex tube and analysis of its flow characteristics, *Int. J. Eng. Technol.* 4 (5) (2018) 45–51.
- [22] Tejshree Bornare, Abhishek Badgujar, Prathamesh Natu, Vortex tube refrigeration system based on compressed air, *Int. J. Mech. Eng. Technol.* 6 (7) (2015) 97–102.
- [23] W. Naksanee, R. Prommas, An experimental investigation on the efficiency of snail entry in vortex tube fed low inlet air pressure to reduce temperature of low pressure air, *Int. J. Heat Technol.* 36 (4) (2018) 1223–1232, <https://doi.org/10.18280/ijht.360409>.
- [24] Chaiyaporn Phankasikorn, Computation of Three Dimensional Flow and Heat Transfer in Vortex Tube, Chulalongkorn University, 2005.
- [25] R. Prommas, P. Rattanadecho, D. Cholaseuk, Energy and exergy analyses in drying process of porous media using hot air, *Int. Commun. Heat Mass Tran.* 37 (2010) 372–378, <https://doi.org/10.1016/j.icheatmasstransfer.2009.12.006>.
- [26] S. Eiamsa-ard, Experimental investigation of energy separation in a counter-flow ranque-hilsch vortex tube with multiple inlet snail entries, *Int. Commun. Heat Mass Tran.* 37 (2010) 637–643, <https://doi.org/10.1016/j.icheatmasstransfer.2010.02.007>.
- [27] Mohammad O. Hamdan, Salah-A.B. Al-Omari, Ali S. Oweimer, Experimental study of vortex tube energy separation under different tube design, *Exp. Therm. Fluid Sci.* 91 (2018) 306–311, <https://doi.org/10.1016/j.expthermflusci.2017.10.034>.
- [28] Aditya Kumar, Sudhakar Subudhi Vivekanand, Cooling and dehumidification using vortex tube, *Appl. Therm. Eng.* 122 (2017) 181–193.
- [29] Eiamsa-ard Smith, Pongjet Promvongse, Review of Ranque–Hilsch effects in vortex tubes, *Renew. Sustain. Energy Rev.* 12 (2008) 1822–1842, <https://doi.org/10.1016/j.rser.2007.03.006>.
- [30] K. Kiran Kumar Rao, Dr G. Sharanappa, Dr A. Ramesh, Experimental analysis of vortex tube by using different materials, *Int. J. Mech. Eng. Technol.* 9 (9) (2018) 1173–1181.

- [31] G.G. Jacobs, L. Liebenberg, The influence of timed coolant injection on compressor efficiency, *Sustain. Energy Tech. Assess.* 18 (2016) 175–189, <https://doi.org/10.1016/j.seta.2016.10.010>.
- [32] Ashraf Elfasakhany, Improving performance and development of two-stage reciprocating compressors, *Int. J. Adv. Res. Eng. Technol.* 3 (2) (2012) 119–136.
- [33] Guoa Da, Zhixian Ma, Jili Zhang, Mingsheng Liu, Energy impact of air pre-cooling on screw air compressor, *Procedia Eng.* 205 (2017) 937–944, <https://doi.org/10.1016/j.proeng.2017.10.147>.
- [34] J.P. Holman, *Experimental Method for Engineers*, sixth ed., McGraw-Hill Co., Singapore, 1994.